

Supporting Information

for

Folate Receptor-targeted Aggregation-enhanced Near-IR Emitting Silica Nanoprobe for One-photon *in vivo* and Two-photon *ex vivo* Fluorescence Bioimaging

Xuhua Wang,[†] Alma R. Morales,[†] Takeo Urakami,[§] Lifu Zhang,^{†‡} Mykhailo V.

Bondar[⊥], Masanobu Komatsu,[§] and Kevin D. Belfield^{†‡}*

[†] Department of Chemistry University of Central Florida, Orlando, FL 32816,

USA

[‡] CREOL, The College of Optics and Photonics, University of Central Florida,

Orlando, FL 32816, USA

[§] Sanford-Burnham Medical Research Institute at *Lake Nona*

Orlando, FL 32827, USA

[‡] School of Electrical Engineering, Anhui Polytechnic University, Wuhu, 241000, China

[⊥] Institute of Physics, Prospect Nauki, 46, Kiev-28, 03094 Ukraine

Table of Contents

| | |
|--|----|
| Table of Contents..... | 2 |
| List of Figures..... | 2 |
| 1. Synthesis of 2-(2,6-bis((E)-2-(7-(diphenylamino)-9,9-diethyl-9H-fluoren-2-yl)vinyl)-4H-pyran-4-ylidene)malononitrile (DFP)..... | 4 |
| 2. Preparation of DFP organic nanoparticles..... | 4 |
| 3. Preparation of (S)-2-(2-(4-((2-amino-4-hydroxypteridin-6-yl)methylamino)phenyl)acetamido)-5-(2-mercaptoethylamino)-5-oxopentanoic acid (FA-SH)..... | 6 |
| 4. Spectroscopic measurements and quantum yield determination..... | 7 |
| 5. Two-photon absorption cross section determination..... | 7 |
| 6. Photostability measurement..... | 8 |
| 7. Cytotoxicity Assay..... | 9 |
| References | 23 |

List of Figures

| | |
|---|----|
| Figure S1. TEM image of DFP nanoparticles obtained from nanoparticle suspension containing 80% volume fraction of water in THF, Scar bar: 100 nm..... | 5 |
| Figure S2. a) UV-vis absorption spectral changes of DFP (5×10^{-6} mol·L ⁻¹) as a function of the water fraction in THF; b) fluorescence emission spectral changes of DFP (5×10^{-6} mol·L ⁻¹) as a function of the water fraction in THF..... | 5 |
| Figure S3. Photobleaching of SNP-DPF-PEGFA and DFP encapsulated in Tween-80 micelles in PBS at 501 nm with a power of 10 mW..... | 9 |
| Figure S4. Viability of HeLa and MG63 cells incubated with SNP-DFP-PEGFA. Error bars represent standard error of the mean of 3 replicates..... | 10 |
| Figure S5. A representative TEM image (a) and DLS size distribution (b) of the FA conjugated nanoparticles in PBS..... | 10 |
| Figure S6. Standard samples with different concentration of SNP-DFP-NH ₂ in PBS (1, 0.5, 0.1, 0.01, and 0.001 μ M). Filter sets for the images of standard samples in tubes are: left 500/720 and right 605/720..... | 11 |
| Figure S7. <i>Ex vivo</i> images of the HeLa tumor and organs of the mice injected with (a) SNP-DFP-PEGFA and (b) SNP-DFP-PEGMAL..... | 11 |

| | |
|---|----|
| Figure S8. One-photon confocal images of HeLa tumor tissue sections (~20 μm thick sections) from mice tail vein injected with SNP-DFP-PEGMAL (3 nmol/g body weight, 6 h p.i.); a) bright field, b) image of the nuclei of the tumor stained with Hoechst 33285 (0.2 $\mu\text{g}/\text{mL}$), Ex: 405 nm, Em: 520 – 560 nm, DM: RSP500 nm; c) image of tumor with the channel for SNP-DFP-PEGFA, Ex: 476 nm, Em: 620 - 680 nm, DM: RSP 500 nm; and d) merged image; objective 63 \times , NA: 1.4. Representative fields from multiple sections of two tumors are shown. | 12 |
| Figure S9. One-photon confocal images of HeLa tumor (~ 20 μm sections) from mice tail vein injected with SNP-DFP-PEGFA (3 nmol/g body weight, 6 h p.i.); a) image of the CD31, primary antibody MEC13.3 (1 : 50 dilution in PBS), secondary antibody Alexa Fluor 350 goat anti-mouse IgG antibody (1 $\mu\text{g}/\text{mL}$), Ex: 351nm, Em: 450 – 560 nm; b) image of tumor with the channel for SNP-DFP-PEGFA, Ex: 476 nm, Em: 620 - 680 nm, DM: RSP 500 nm; c) merged image; Objective 10 \times , NA: 0.4; Representative fields from multiple sections of two tumors are shown. | 13 |
| Figure S10. Representative thick 3D-two-photon fluorescence image of the HeLa tumor from a mouse that was injected with SNP-DFP-PEGMAL (3 nmol/g) into the tail vein. Ex: 980 nm; Power: 300 mW, ~20% on the focal plane; short-pass filter 840 nm, 20 \times (N.A. 1.0, Leica). | 14 |
| Figure S11. ^1H NMR spectra of FA-SH in DMSO-6d. | 15 |
| Figure S12. ^1H NMR spectra of SCM-PEG-MAL in D_2O | 16 |
| Figure S13. ^1H NMR spectra of Tween-80 in D_2O | 17 |
| Figure S14. ^1H NMR spectra of DFP in CDCl_3 | 18 |
| Figure S15. ^1H NMR spectra of SNP-DFP- NH_2 in D_2O | 19 |
| Figure S16. ^1H NMR spectra of SNP-DFP-PEGMAL in D_2O | 20 |
| Figure S17. ^1H NMR spectra of SNP-DFP-PEGFA in D_2O | 21 |
| Figure S18. Stacked plot of the ^1H NMR spectra of the materials. | 22 |

1. Synthesis of 2-(2,6-bis((E)-2-(7-(diphenylamino)-9,9-diethyl-9H-fluorene-2-yl)vinyl)-4H-pyran-4-ylidene)malononitrile (DFP).

A mixture of 7-(diphenylamino)-9,9-diethyl-9H-fluorene-2-carbaldehyde (0.6 g, 1.43 mmol), and commercial 2,6-dimethyl-4-dicyanomethylene-4H-pyran (0.13 g, 0.71 mmol) were dissolved in EtOH (35 mL). After adding piperidine (0.4 mL) slowly via syringe while stirring, the reaction mixture was refluxed for 72 h. Reddish precipitate was obtained after cooling the reaction to room temperature. DFP was obtained after purifying the product through a silica gel column using hexanes/ethyl acetate (4:1) as eluent. A red solid was obtained (0.35 g, 25% yd); m.p. 229-230 °C. ¹H NMR (300 MHz, CDCl₃) δ: 7.68 (s, 1H), 7.66 (s, 2H), 7.60-7.52 (m, 8H), 7.30-7.24 (m, 10H), 7.15-7.10 (m, 10H), 7.06-7.01 (m, 5H) 6.84 (s, 1H), 6.79 (s, 1H), 6.72 (s, 2H), 2.01-1.94 (m, 8H), 0.39 (t, J = 14.7 Hz, 12H). ¹³C NMR (75 MHz, CDCl₃) δ: 158.6, 155.8, 152.0, 150.8, 148.2, 147.7, 144.2, 138.6, 135.1, 132.5, 129.2, 127.8, 124.2, 1232.2, 122.9, 121.6, 121.0, 119.5, 118.6, 117.1, 115.4, 106.8, 59.0, 56.1, 32.6, 8.6. HRMS-ESI theoretical m/z [M+H]⁺ = 971.47, found, 971.46, theoretical; m/z [2M+H]⁺ = 1941.93, found, 1941.92, theoretical.

2. Preparation of DFP organic nanoparticles.

The DFP organic nanoaggregate dispersion was prepared by injecting a 0.125 mL stock solution of DFP in THF (2×10^{-4} M) into 4.825 mL of a THF/water mixture, with vigorous stirring. In all samples, the final concentration of DFD (5×10^{-6} M) was constant after stock solution injection. The relative fluorescence quantum yield values of those were measured at the same concentration of 5×10^{-6} M.

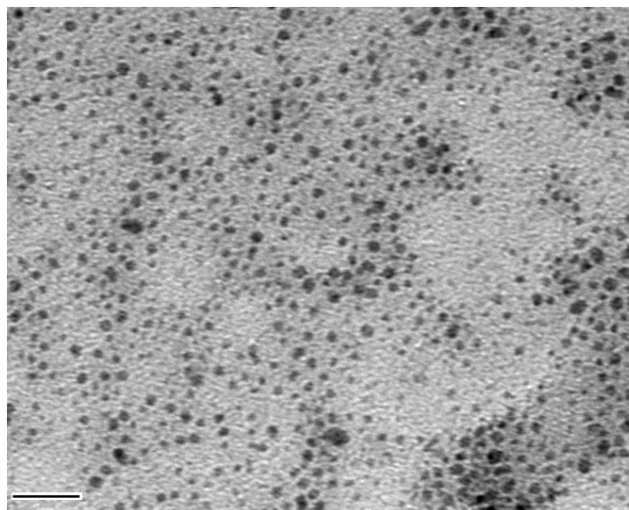


Figure S1. TEM image of DFP nanoparticles obtained from nanoparticle suspension containing 80% volume fraction of water in THF, Scar bar: 100 nm.

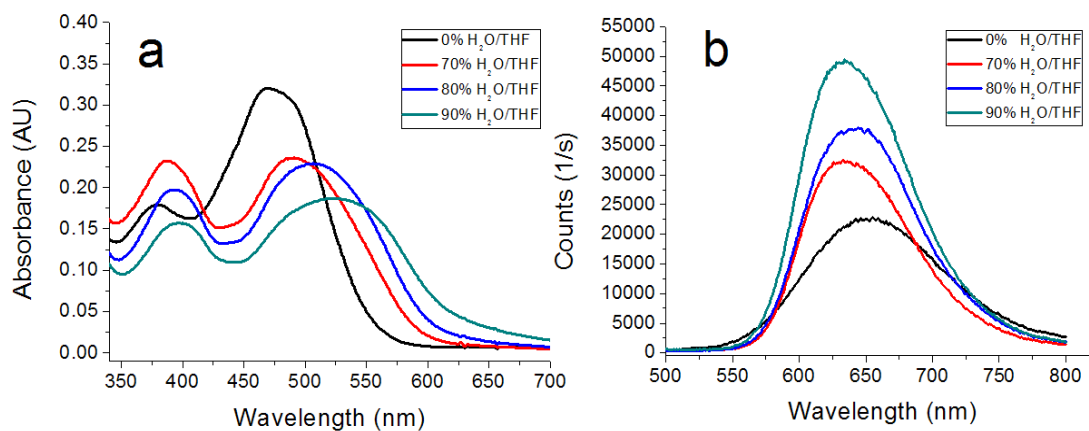
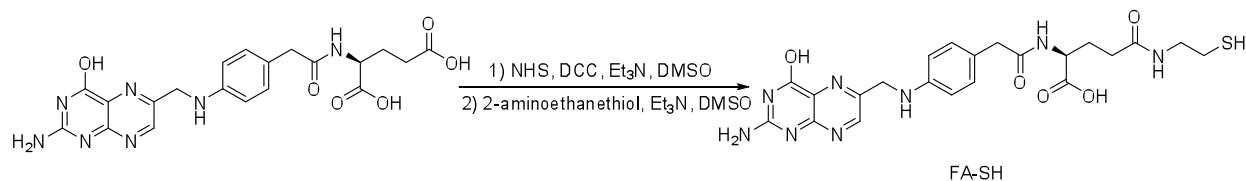


Figure S2. a) UV-vis absorption spectral changes of DFP ($5 \times 10^{-6} \text{ mol}\cdot\text{L}^{-1}$) as a function of the water fraction in THF; b) fluorescence emission spectral changes of DFP ($5 \times 10^{-6} \text{ mol}\cdot\text{L}^{-1}$) as a function of the water fraction in THF.

3. Preparation of (*S*)-2-(2-(4-((2-amino-4-hydroxypteridin-6-yl)methylamino)phenyl)acetamido)-5-(2-mercaptoethylamino)-5-oxopentanoic acid (FA-SH)



N-Hydroxysuccinimide ester of folic acid (NHS-FA (γ)) was prepared in accordance to a reported procedure.¹ Briefly, folic acid (1.0 g, 2.2 mmole) was added into a mixture of anhydrous dimethyl sulfoxide (DMSO, 30 mL) and triethylamine (TEA, 0.5 mL, 3.6 mmol). Folic acid dissolved while stirring the mixture under nitrogen and in the dark overnight. Folic acid was mixed with dicyclohexylcarbodiimide (DCC, 0.5 g, 2.4 mmole) and *N*-hydroxysuccinimide (NHS, 0.52 g, 4.5 mmole), and stirred in the dark for a further 18 h. The side product, dicyclohexylurea (DCU), precipitated and was removed by vacuum filtration. An equimolar amount of 2-aminoethanethiol (0.170 g, 2.2 mmole) and 10 mL TEA was added to the filtrate, and the reaction was conducted under nitrogen overnight. Subsequently, 30 mL CH₂Cl₂ and 30 mL hexanes were added to the reaction mixture to precipitate the crude product that was collected by filtration. The crude product was then dissolved in 30 mL water whose pH was adjusted to 10.0 by ammonium hydroxide. The solution was washed thrice with CH₂Cl₂. After neutralization with HCl, the yellow product was precipitated and collected by filtration; 66% yd; m.p. dec at 187 °C. ¹H NMR (d-DMSO, 300 MHz) δ (TMS ppm): 12.27 (b, COOH, 1H), 8.64 (s, pteridine moiety, 1H), 8.05- 8.23 (b, NH-CO, 2H), 7.66 (d, Ar ring, 2H), 7.20 (b, NH₂, 2H), 6.65 (d, Ar ring, 2H), 4.51 (d, CH₂-N, 2H), 4.27 (m, NCH-CO-, 1H), 3.31 (t, N-CH₂, 2H), 2.74 (t, CH₂-S, 1H), 2.20 (m, CH₂, 2H), 1.90-2.16 (m, CH₂, 2H, SH, 1H).

4. Spectroscopic measurements and quantum yield determination.

Steady-state absorption spectra were obtained with an Agilent 8453 UV-vis spectrophotometer in 10 mm path length quartz cuvettes. Steady-state fluorescence emission spectra and fluorescence quantum yield measurements were carried out using a PTI QuantaMaster spectrofluorimeter. The fluorescence quantum yields were recorded by using cresyl violet in methanol ($\Phi_f = 0.54$)² as standard since its emission was similar to DFP. The optical density of the standard was less than 0.1. The values of fluorescence quantum yields, $\Phi_{f(\text{sample})}$, were calculated according to equation 1:

$$\Phi_{f(\text{sample})} = \Phi_{f(\text{ref})} \frac{OD_{(\text{ref})} I_{(\text{sample})} n_{(\text{sample})}^2}{OD_{(\text{sample})} I_{(\text{ref})} n_{(\text{ref})}^2} \quad (1)$$

where Φ_f is the quantum yield, I is integrated emission signal, OD is optical density at the excitation wavelength, and n is the refractive index; subscript 'ref' stands for standard (reference sample), 'sample' stands for samples (DFP).

5. Two-photon absorption cross section determination.

The 2PA spectra of DFP in THF and CHCl_3 and 20 wt% SiNPs (SNP-DFP-PEGMAL) in PBS, were determined over a broad spectral region by a typical z-scan method.³ We used a femtosecond regenerative Ti:sapphire amplifier (Coherent Legend-HE), which is seeded by a Ti:sapphire femtosecond oscillator (Coherent Mira 900). An optical parametric amplifier (OPA) (Coherent OperA-Solo) pumped by the Coherent Legend-HE provided laser pulses of 100 fs duration with a broadly adjustable wavelength. The tuning range of 700–1200 nm was used in this experiment. The z-scan measurements were performed in 1 mm quartz cuvettes with DFP at

$\sim 10^{-2}$ M in THF and SNP-DFP-PEGMAL at $\sim 3 \times 10^{-4}$ M in PBS. In addition, the scattering affect of the nanoparticles was checked by non-dye labeled nanoparticles with the same concentration and no significant signal was observed from the blank particles at this concentration. The uncertainty in the measured cross sections was ca. 15%.

6. Photostability measurement.

The photostability of dye-doped SiNPs and free dye DFP encapsulated in Tween-80 micelles in PBS were determined by the absorption method previously described.⁴ A solution of SNP-DFP-PEGFA in PBS or DFP encapsulated in Tween-80 micelles in PBS was irradiated in 1 cm path length quartz cuvettes with a 501 nm Argon laser at 10 mW. The values of photodecomposition quantum yields, Φ_d , were calculated according to equation 2, and the results are the average of ten pairs of adjacent absorbance maxima. The normalized absorbance maxima of two solutions according to the bleaching time are presented in Figure S3,

$$\Phi_d = \frac{(A_1 - A_0)N_A}{10^3 \times \varepsilon \times I \times (1 - 10^{-(A_1 + A_0)/2})(t_1 - t_0)} \quad (2)$$

where Φ_d is the photobleaching decomposition quantum yield, A_1 is absorbance maxim at t_1 , A_0 is absorbance max at t_0 , N_A is Avogadro's number, ε is molar absorbance, $t_1 - t_0$ is time exposed (s), and I is the intensity of laser in $\text{photon} \cdot \text{cm}^{-2} \cdot \text{s}^{-1}$.

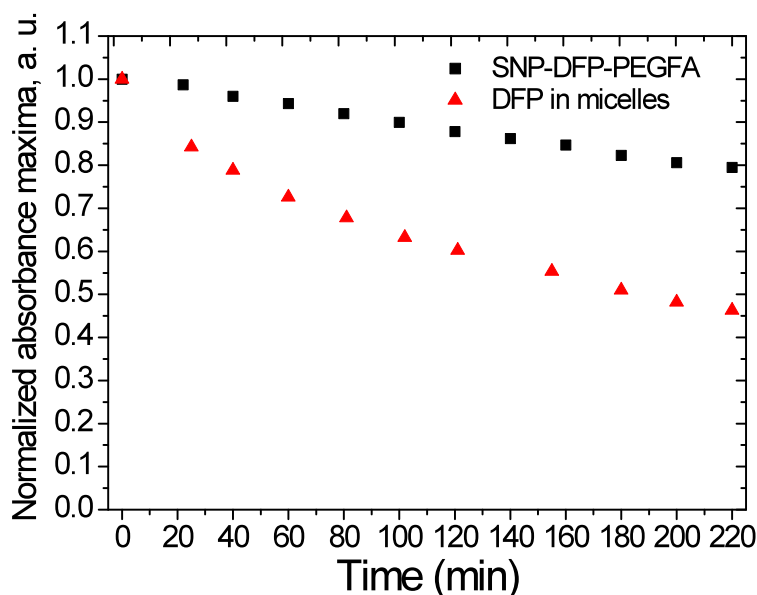


Figure S3. Photobleaching of SNP-DPF-PEGFA and DFP encapsulated in Tween-80 micelles in PBS at 501 nm with a power of 10 mW.

7. Cytotoxicity Assay.

To assess the cytotoxicity of silica nanoprobe, 1×10^3 per well of HeLa or MG63 cells in 96-well plates were incubated in 90 μL of RPMI-1640 medium without phenol red, supplemented with 10% FBS and 100 units/mL penicillin-streptomycin for 24 h. The cells were then incubated with various amounts of SiNPs containing a certain amount of DFP (0.01, 0.1, 0.5, 1, and 5 μM) for an additional 20 h. Subsequently, 20 μL of CellTiter 96[®] AQueous One Solution reagent was added to each well, followed by further incubation for 4 h at 37 °C. The relative viability of the cells incubated with the silica nanoprobe to untreated cells was determined by measuring the MTS-formazan absorbance on a microplate reader (Spectra Max M5, Molecular Devices, Sunnyvale, CA, USA) at 538 nm with subtraction of the absorbance of the cell-free nanoprobe at

538 nm. The results from three individual experiments were averaged. The cell viability data are presented in Figure S4.

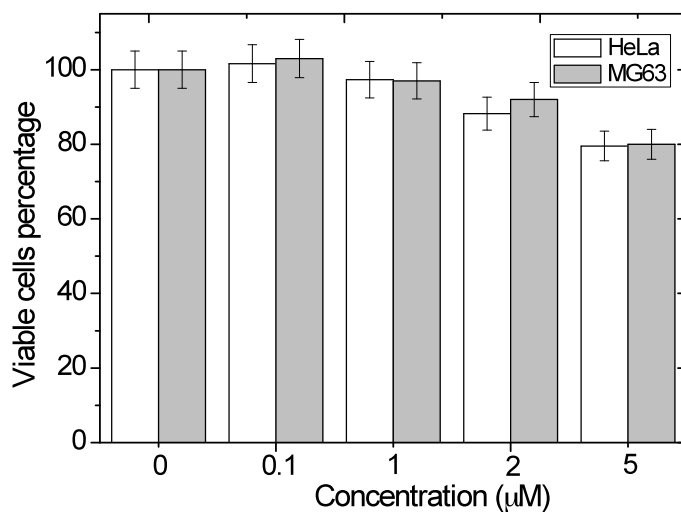


Figure S4. Viability of HeLa and MG63 cells incubated with SNP-DFP-PEGFA. Error bars represent standard error of the mean of 3 replicates.

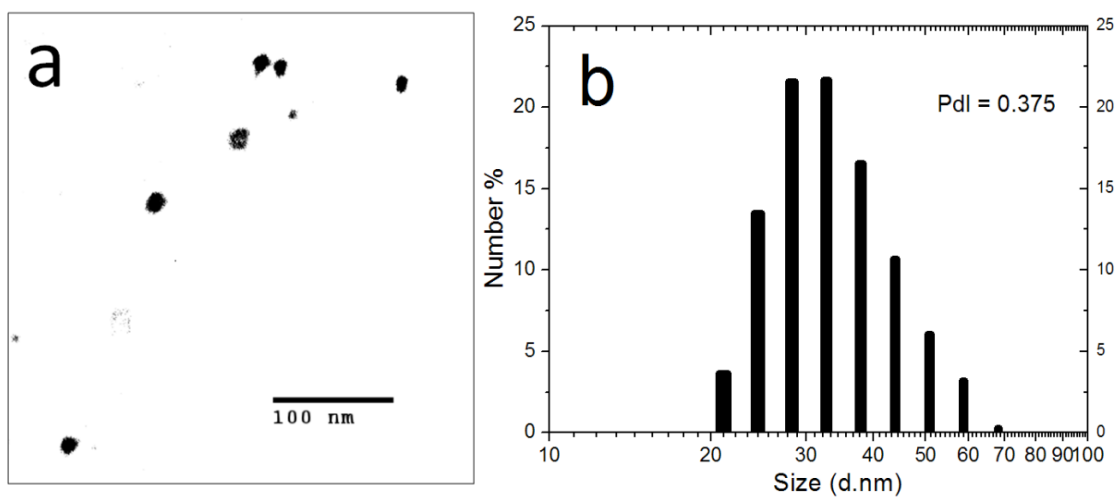


Figure S5. A representative TEM image (a) and DLS size distribution (b) of the FA conjugated nanoparticles in PBS.

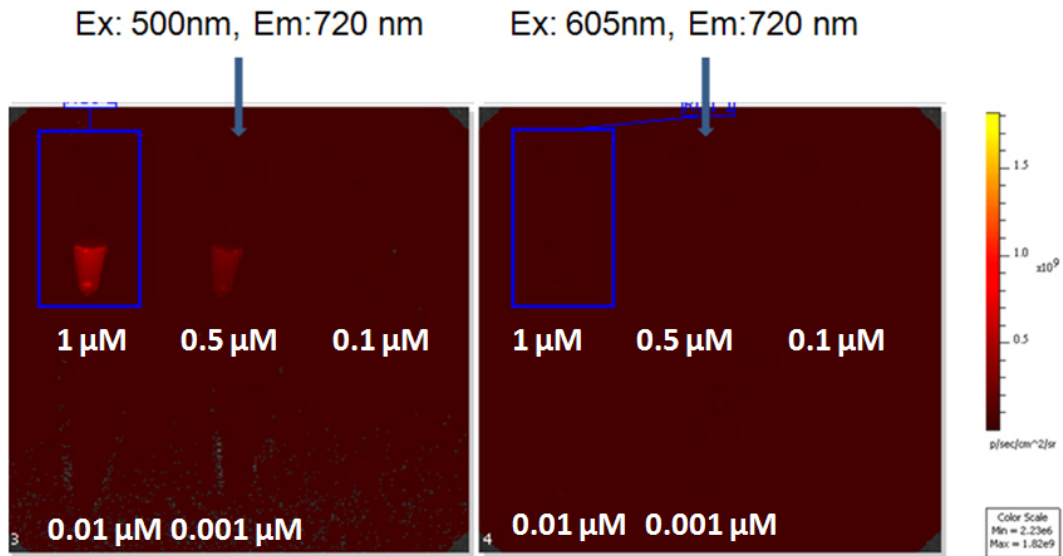


Figure S6. Standard samples with different concentration of SNP-DFP-NH₂ in PBS (1, 0.5, 0.1, 0.01, and 0.001 μM). Filter sets for the images of standard samples in tubes are: left 500/720 and right 605/720.

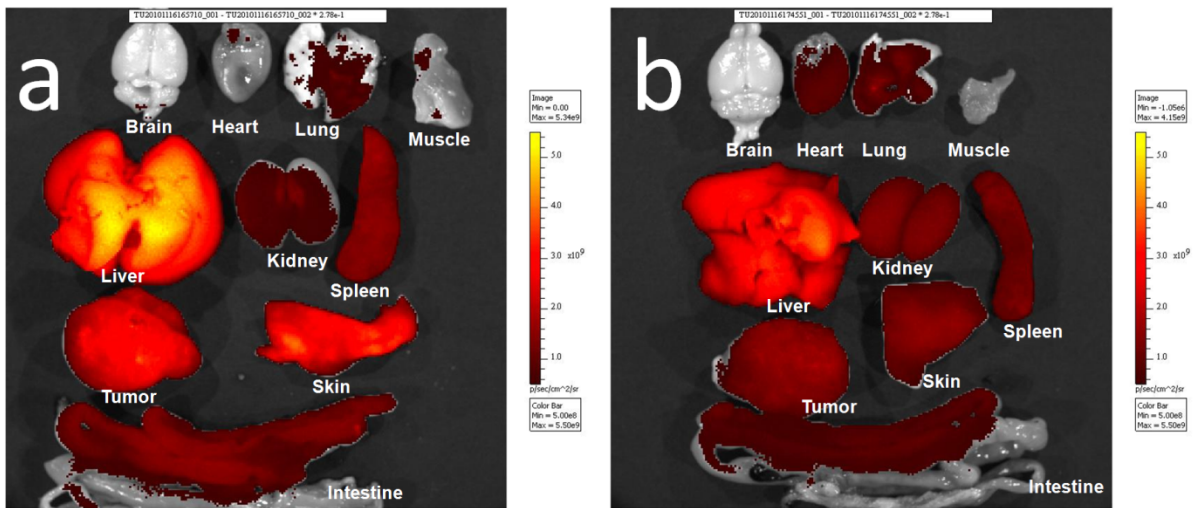


Figure S7. *Ex vivo* images of the HeLa tumor and organs of the mice injected with (a) SNP-DFP-PEGFA and (b) SNP-DFP-PEGMAL.

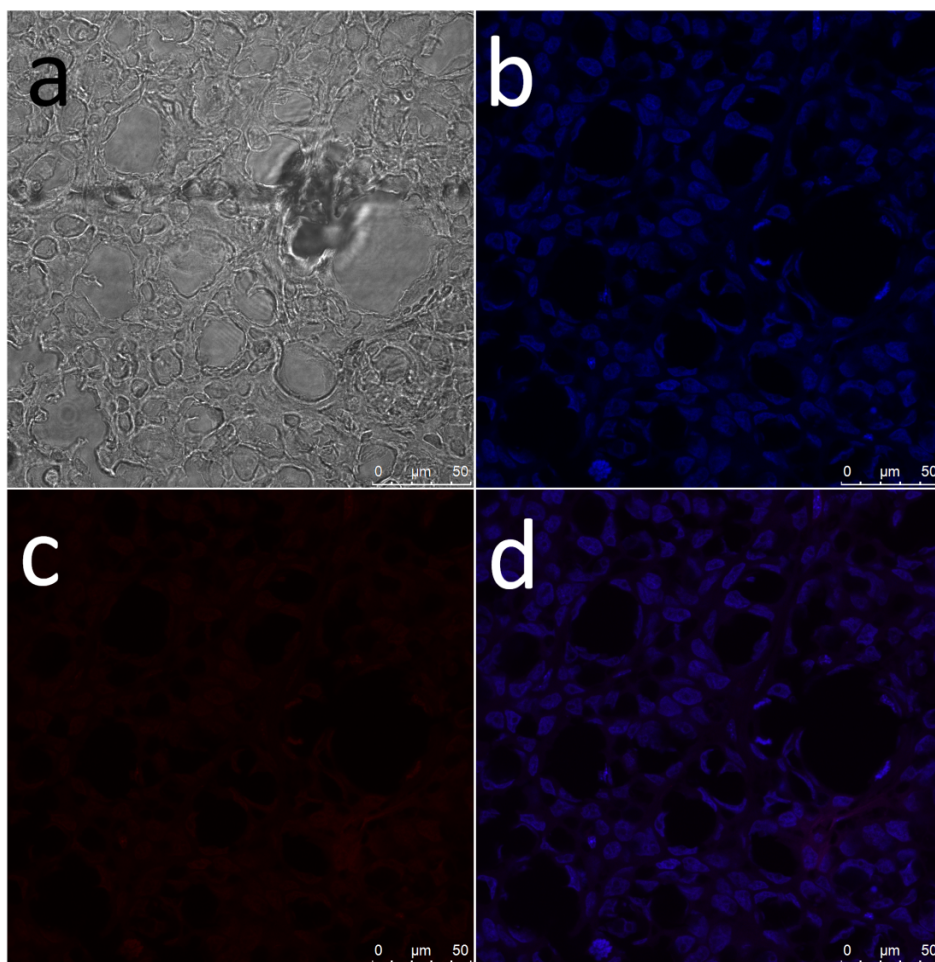


Figure S8. One-photon confocal images of HeLa tumor tissue sections ($\sim 20 \mu\text{m}$ thick sections) from mice tail vein injected with SNP-DFP-PEGMAL (3 nmol/g body weight, 6 h p.i.); a) bright field, b) image of the nuclei of the tumor stained with Hoechst 33285 (0.2 $\mu\text{g}/\text{mL}$), Ex: 405 nm, Em: 520 – 560 nm, DM: RSP500 nm; c) image of tumor with the channel for SNP-DFP-PEGFA, Ex: 476 nm, Em: 620 - 680 nm, DM: RSP 500 nm; and d) merged image; objective 63 \times , NA: 1.4. Representative fields from multiple sections of two tumors are shown.

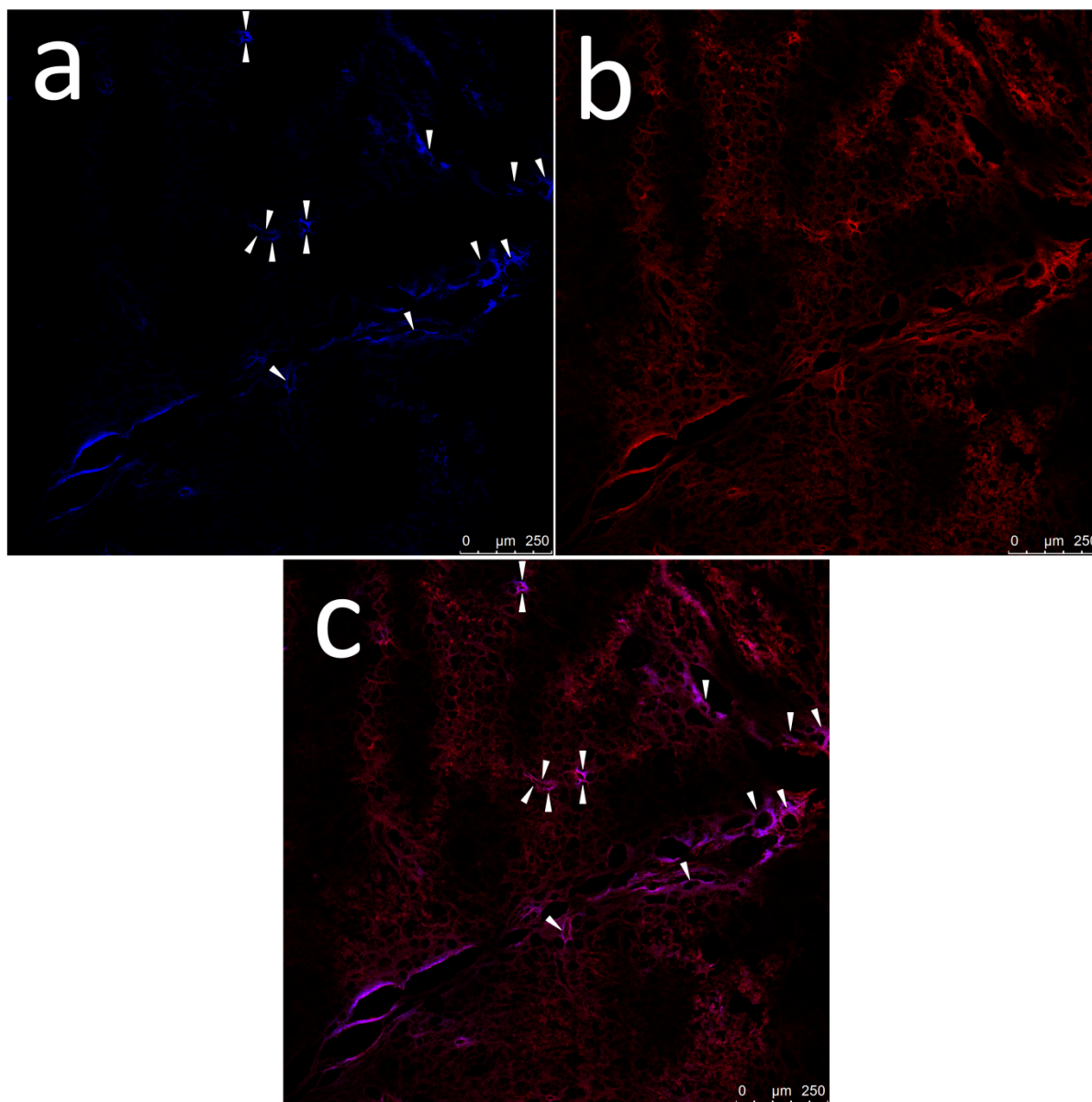


Figure S9. One-photon confocal images of HeLa tumor ($\sim 20 \mu\text{m}$ sections) from mice tail vein injected with SNP-DFP-PEGFA (3 nmol/g body weight, 6 h p.i.); a) image of tumor vessels stained for CD31, primary antibody MEC13.3 (1 : 50 dilution in PBS), secondary antibody Alexa Fluor 350 goat anti-mouse IgG antibody (1 $\mu\text{g}/\text{mL}$), Ex: 351nm, Em: 450 – 560 nm; b) image of tumor with the channel for SNP-DFP-PEGFA, Ex: 476 nm, Em: 620 - 680 nm, DM: RSP 500 nm; c) merged image; Objective 10 \times , NA: 0.4; Representative fields from multiple sections of two tumors are shown.

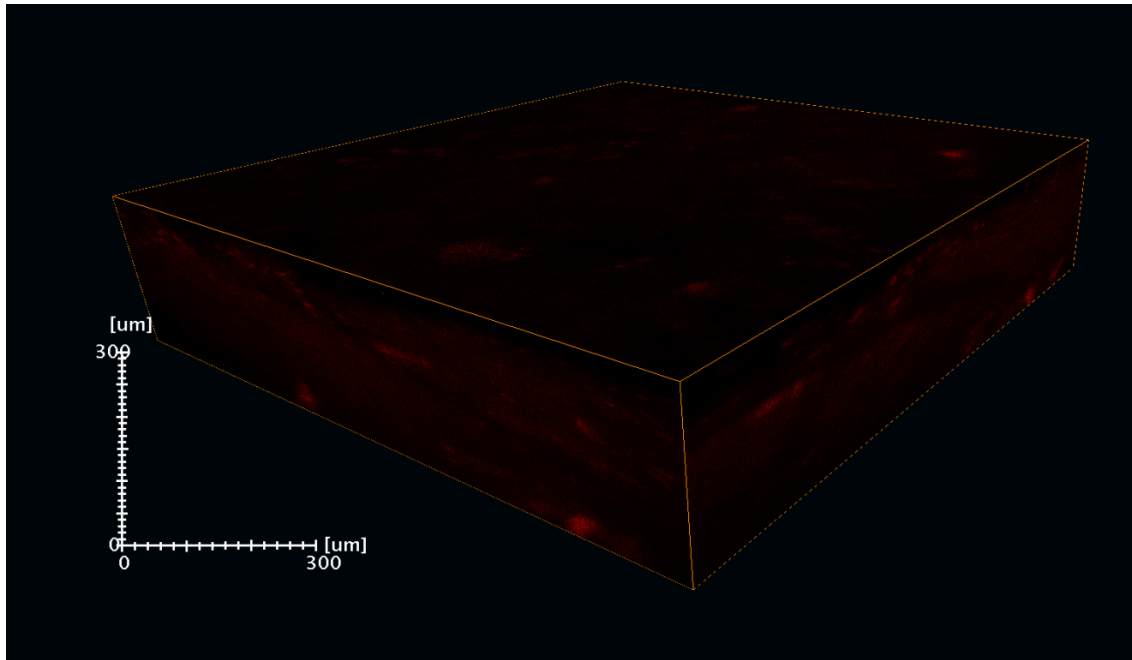


Figure S10. Representative thick 3D-two-photon fluorescence image of the HeLa tumor from a mouse that was injected with SNP-DFP-PEGMAL (3 nmol/g) into the tail vein. Ex: 980 nm; Power: 300 mW, ~20% on the focal plane; short-pass filter 840 nm, 20× (N.A. 1.0, Leica).

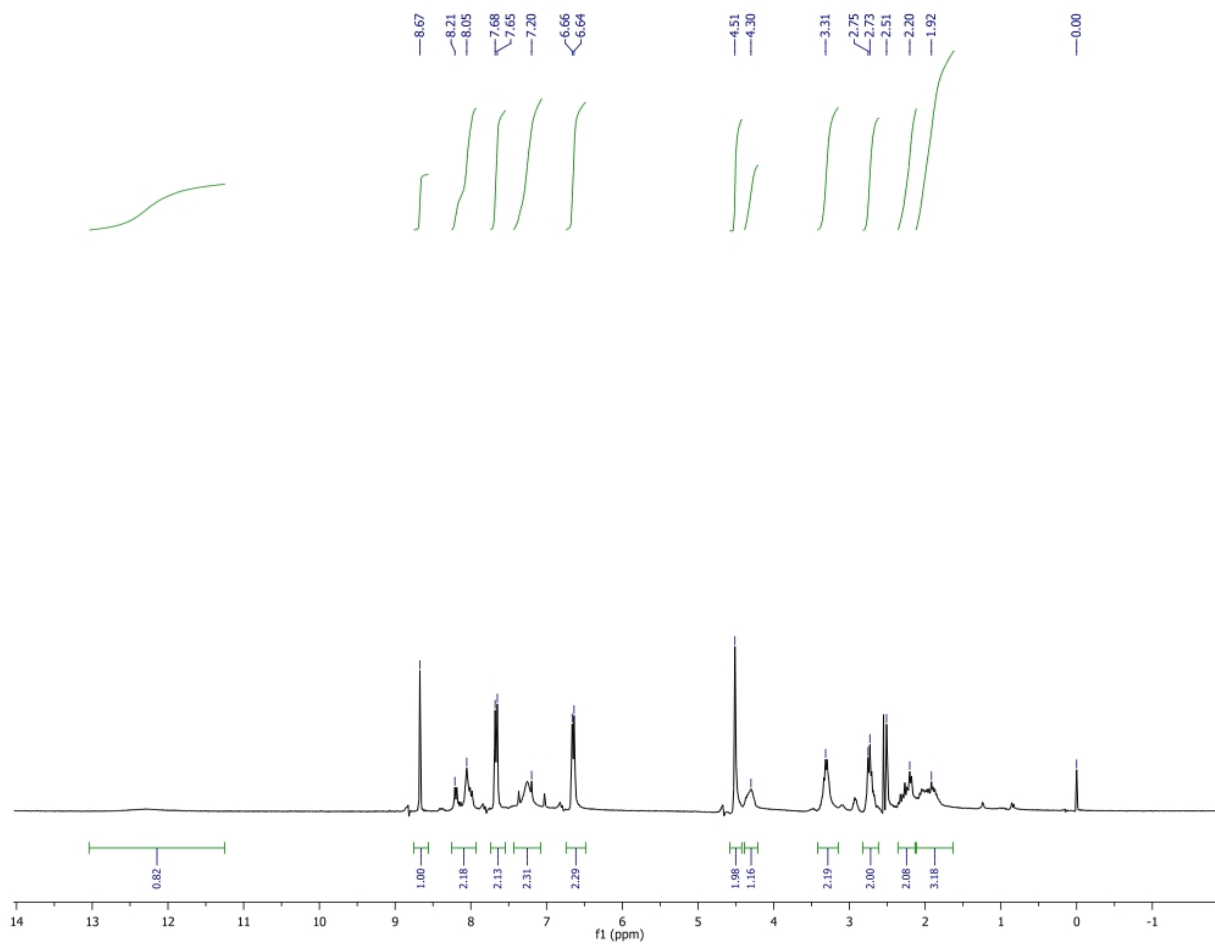


Figure S11. ^1H NMR spectra of FA-SH in DMSO- d_6 .

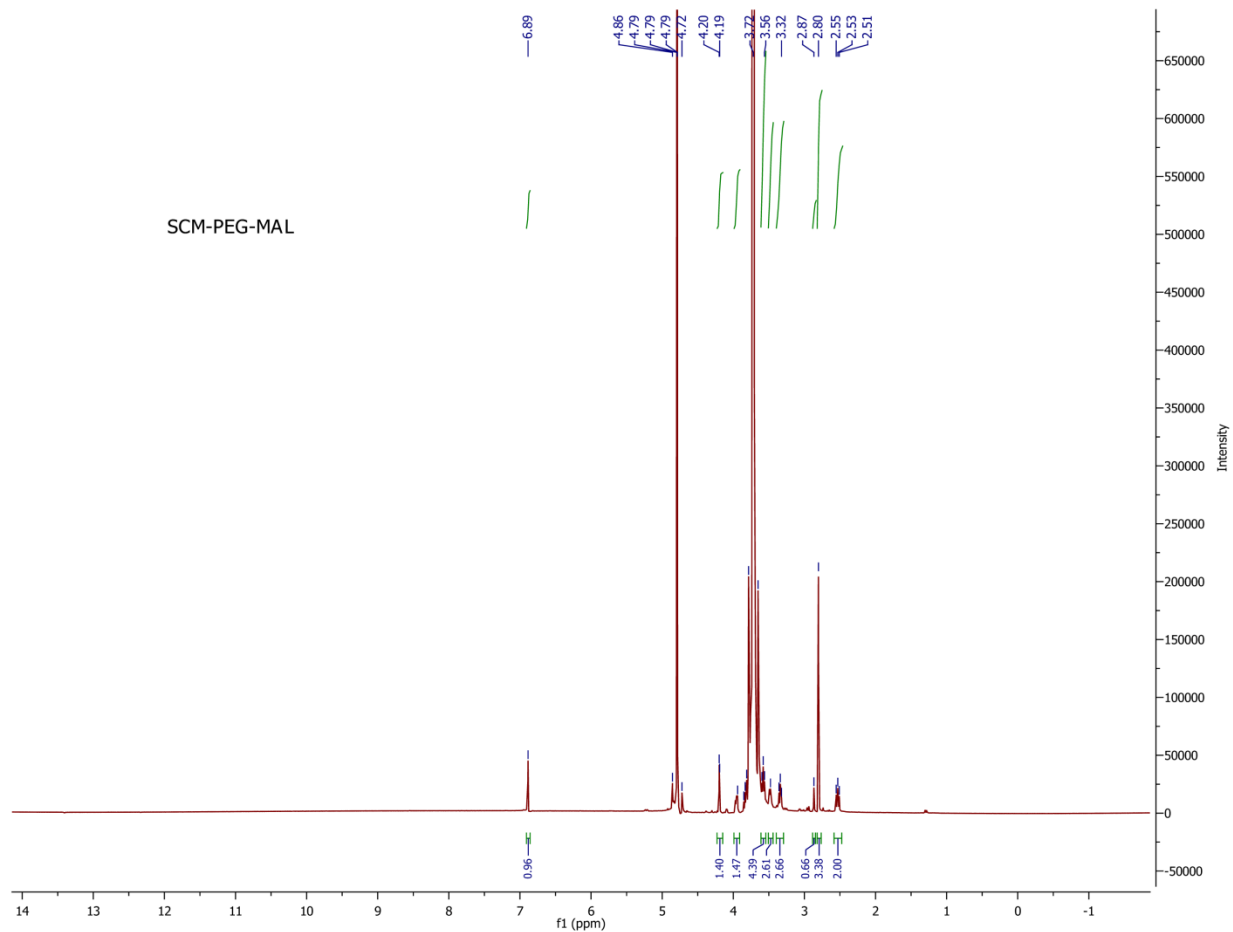


Figure S12. ^1H NMR spectra of SCM-PEG-MAL in D_2O .

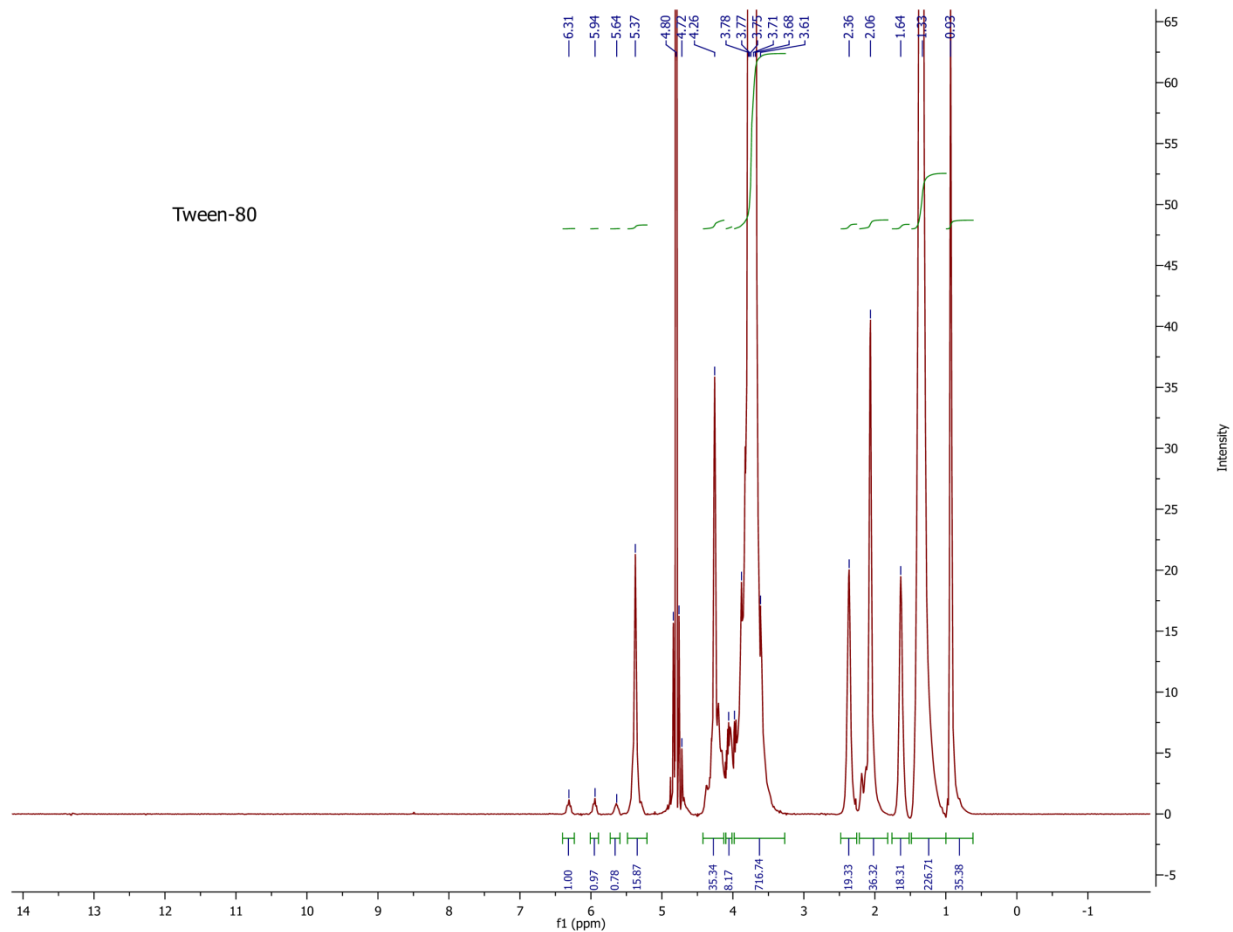


Figure S13. ^1H NMR spectra of Tween-80 in D_2O .

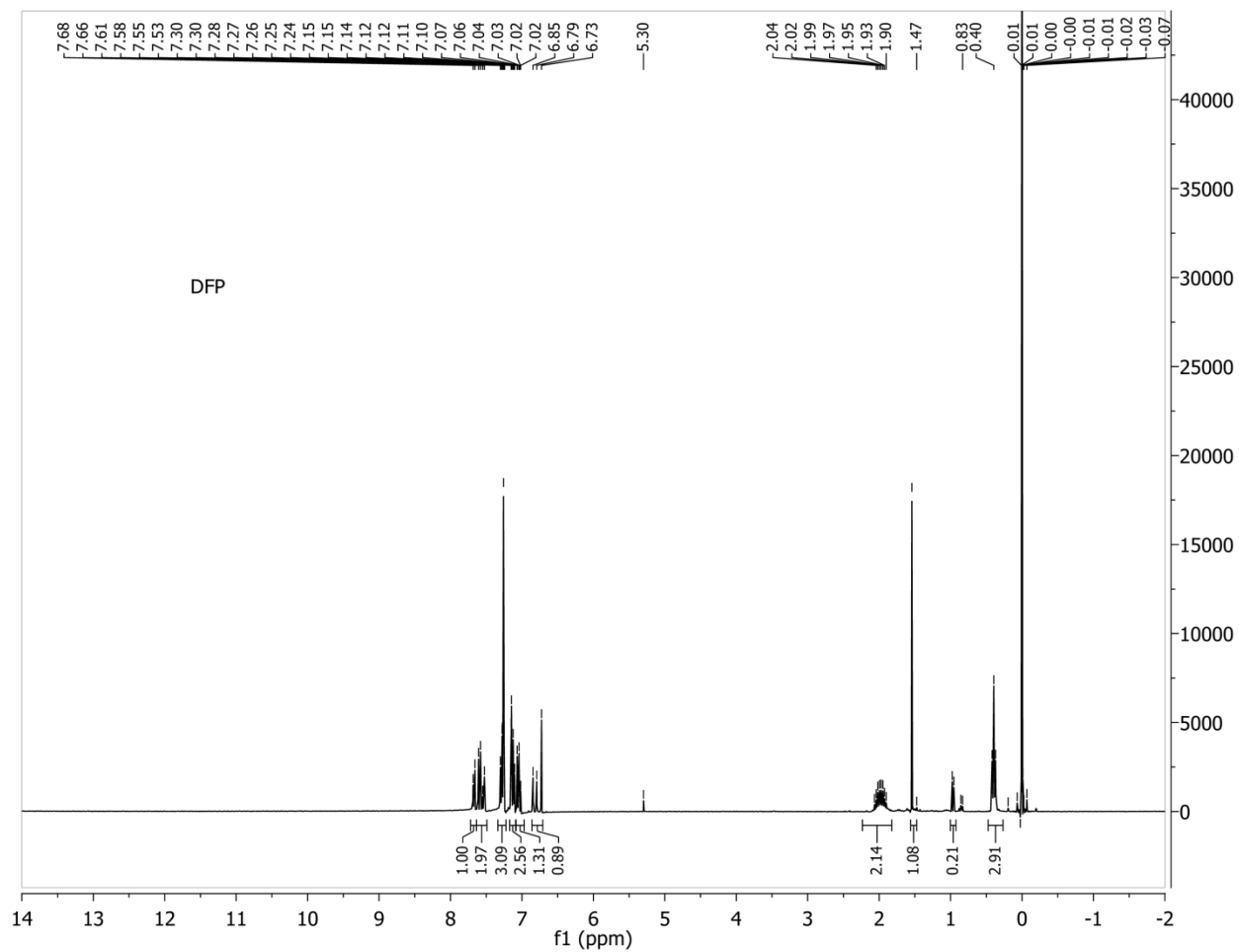


Figure S14. ^1H NMR spectra of DFP in CDCl_3 .

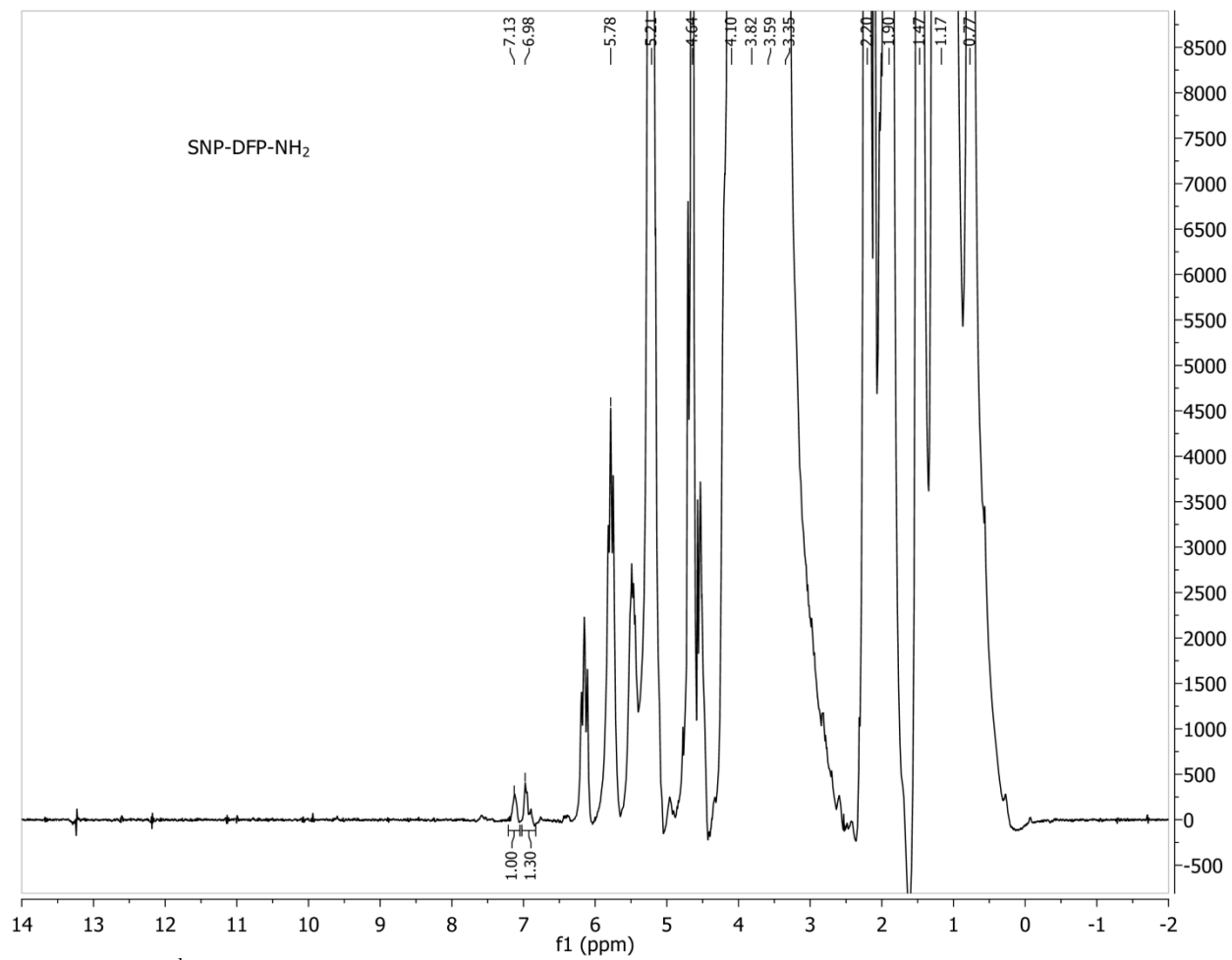


Figure S15. ¹H NMR spectra of SNP-DFP-NH₂ in D₂O.

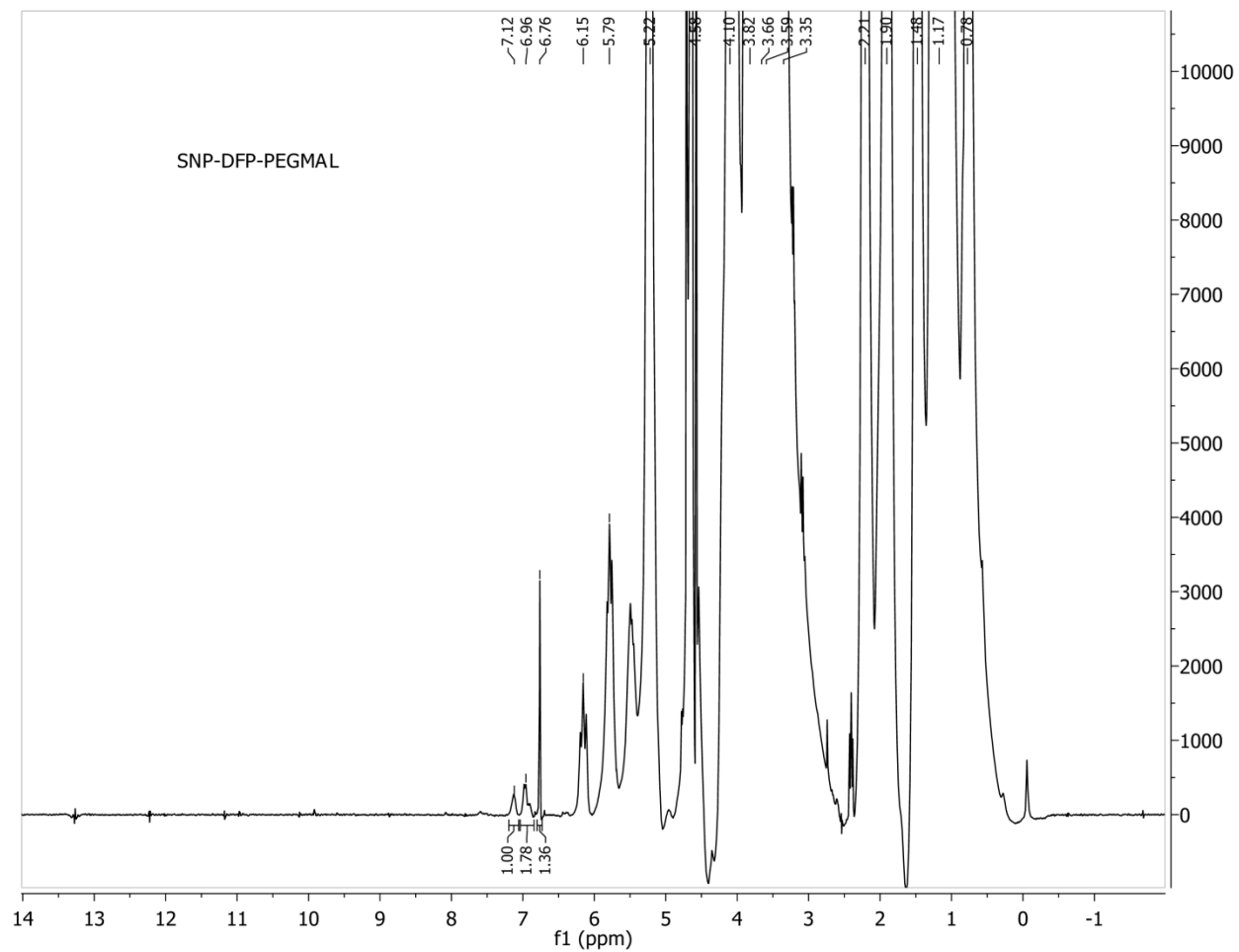


Figure S16. ^1H NMR spectra of SNP-DFP-PEGMAL in D_2O .

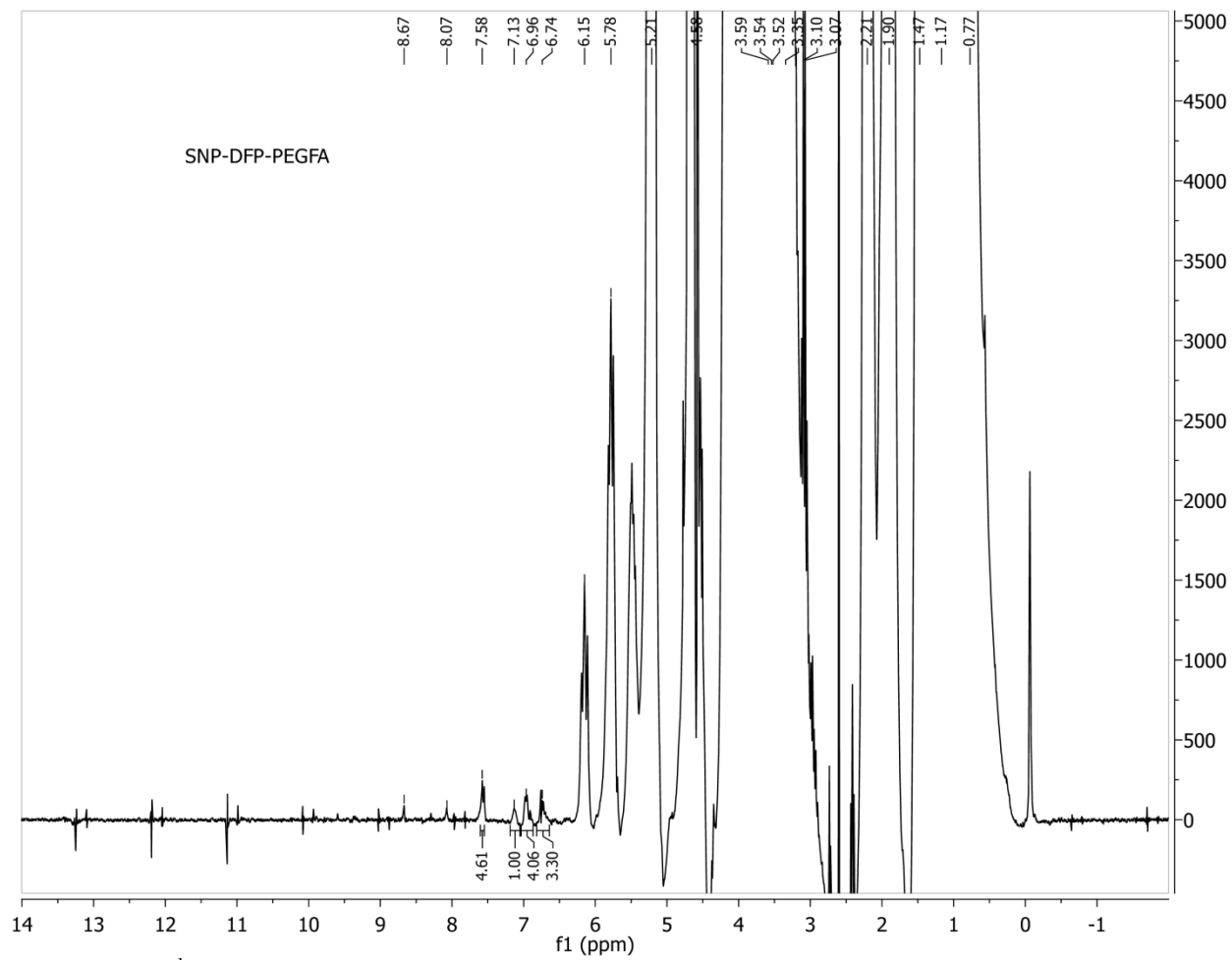


Figure S17. ^1H NMR spectra of SNP-DFP-PEGFA in D_2O .

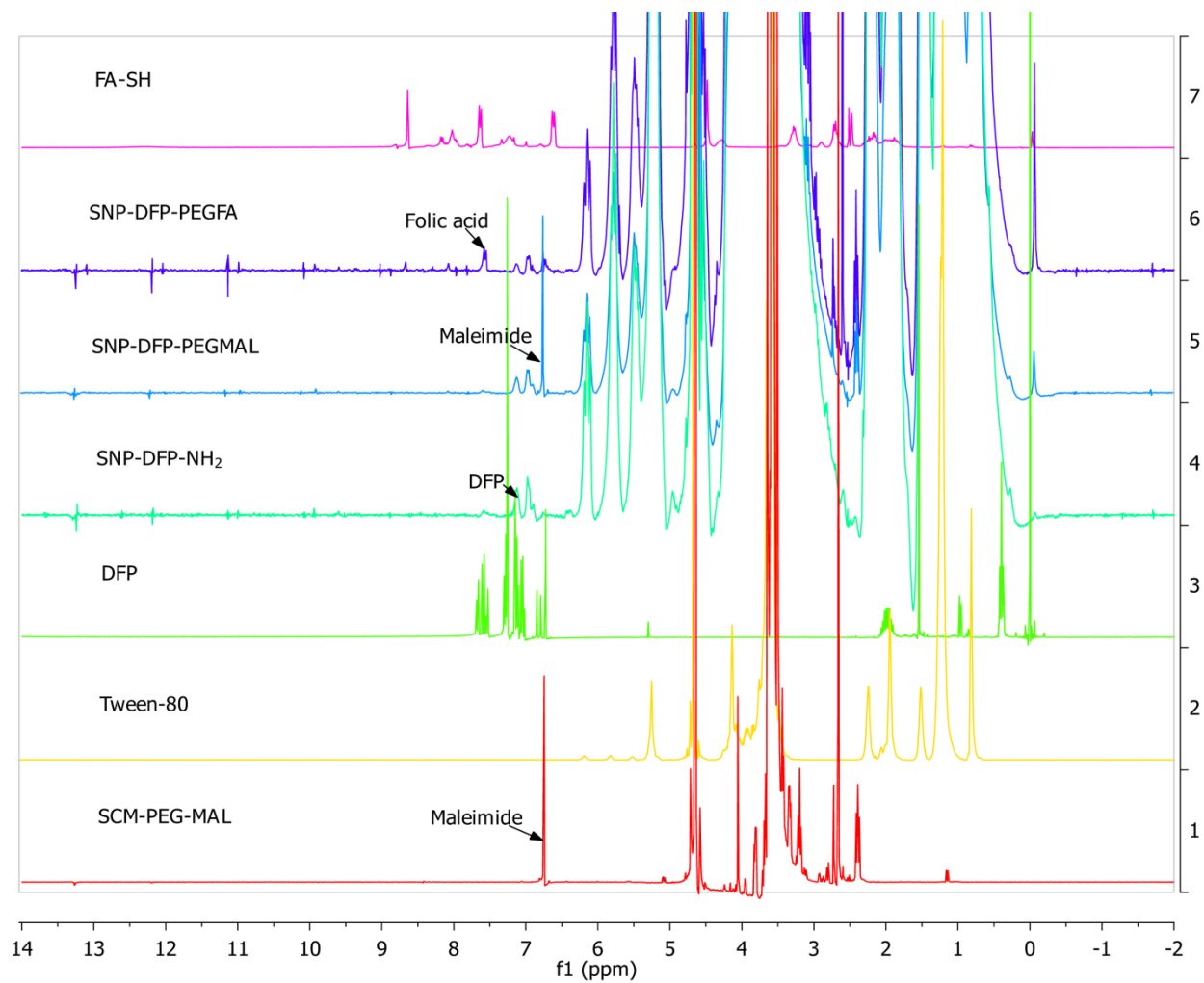


Figure S18. Stacked plot of the ^1H NMR spectra of the materials.

References

- (1) a) Hu, X., Chen, X., Liu, S. Shi, Q., and Jing, X. (2008) Novel aliphatic poly(ester-carbonate) with pendant allyl ester groups and its folic acid functionalization. *J. Polym. Sci. A: Polym. Chem.* 46, 1852-1861. b) Chan, P., Kurisawa, M., Chung, J. E., and Yang, Y. (2007) Synthesis and characterization of chitosan-g-poly(ethylene glycol)-folate as a non-viral carrier for tumor-targeted gene delivery. *Biomaterials* 28, 540-549.
- (2) Lakowicz, J. R. Principles of Fluorescence Spectroscopy, Plenum Press: New York, 1999, pp 53.
- (3) Sheik-Bahae, M., Said, A. A., Wei, T. H., Hagan, D. J., and Van Stryland, E. W. (1990) Sensitive measurement of optical nonlinearities using a single beam. *IEEE J. Quantum Electron.* QE-26, 760–769.
- (4) Corredor, C. C., Belfield, K. D., Bondar, M. V., Przhonska, O. V., and Yao, S. (2006) One- and two-photon photochemical stability of linear and branched fluorene derivatives. *J. Photochem. Photobiol. A: Chem.* 184, 105-112.